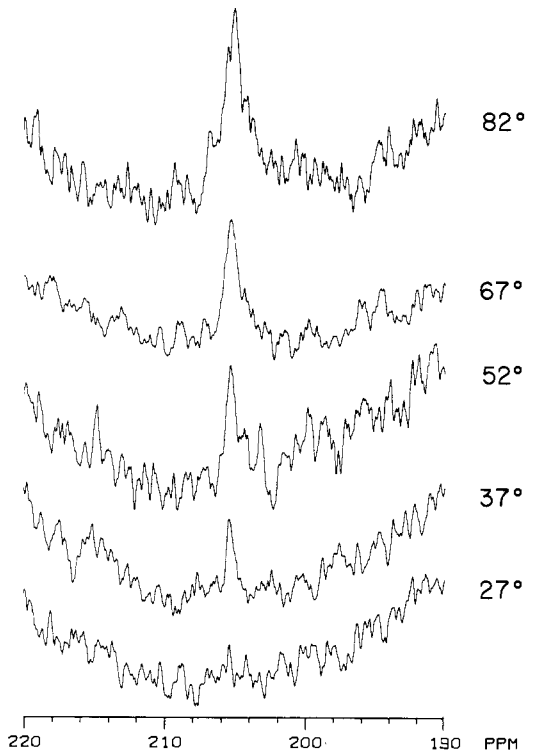

Figure 2. Temperature dependence of the aldehyde region in the proton-decoupled ^{13}C NMR spectrum of D-[1-^{13}C]glucose. Sample and spectral conditions are those of Figure 1, except that the pH was 4.8 for all spectra, the digital Lorentzian broadening was 10 Hz, and the number of 200-scan batches was 101 (27 °C), 177 (37 °C), 113 (52 °C), 376 (67 °C), and 161 (82 °C). Vertical amplitudes have been normalized so that integrated intensities are proportional to aldehyde content.

broadening instead of the 0.5 Hz used for Figure 1. After subtraction of the 10-Hz digital broadening, the line width goes from about 20 Hz at 37 °C to about 70 Hz at 82 °C. It is dominated by the exchange contribution (W_{ex}) from interconversion of aldehyde into all the other tautomers. The other tautomers exhibit relatively small W_{ex} values, but those of the α-furanose and *gem*-diol are measurable. We plan to report on kinetic data extracted from W_{ex} measurements in a future publication.

Integrated intensities yielded the tautomeric composition at temperatures in the range 27-82 °C (Table I). The proportions of the pyranose tautomers are almost independent of temperature; those of the two furanoses and the *gem*-diol increase by a factor of about 5; the proportion of aldehyde increases by an order of magnitude. Our results for the aldehyde are in reasonable agreement with values obtained from circular dichroism spectra by Hayward and Angyal.[19] It is of interest that, within experimental error, we observe equal amounts of α-furanose and β-furanose at all temperatures. About equal proportions of the two furanoses have been observed for 5-*O*-methyl-D-glucose[20] and D-glucose 5,6-carbonate.[21] D-Idose, the other unmodified hexose with a *xylo* configuration, exhibits a β-furanose/α-furanose ratio (structurally analogous to the α-furanose/β-furanose ratio of D-glucose) of 1.2 at 30 °C.[3]

Finally, we wish to comment on the question of artifacts (labeled with X in Figure 1). It is well-known that very large signal-to-noise ratios (for the large resonances) reveal spurious peaks caused by imperfect accumulation and processing.[22-26] We believe that a detailed understanding of the origin of the artifacts will yield methods for reducing their size to levels even lower than in Figure 1 and also systematic procedures for distinguishing residual artifacts from real peaks. One specific procedure applicable to studies of tautomeric composition of monosaccarides is the use of $^1J_{CH}$ values.[3]

Table I. Tautomeric Composition (Percent) of Aqueous D-Glucose[a]

temp, °C	αP	βP	αF	βF	$CH(OH)_2$	CHO
27[b]	38.8	60.9	0.14	0.15	0.0045	c
37[b]	39.4	60.2	0.20	0.21	0.0077	0.0024
37[d]	39.1	60.5	0.19	0.22	0.0062	c
52[b]	39.7	59.7	0.32	0.31	0.0090	0.0051
67[b]	39.9	59.2	0.40	0.46	0.016	0.0096
82[b]	40.1	58.5	0.60	0.69	0.022	0.019

[a] αP, βP, αF, βF, $CH(OH)_2$, and CHO designate α-D-glucopyranose, β-D-glucopyranose, α-D-glucofuranose, β-D-glucofuranose, the *gem*-diol tautomer, and the aldehyde tautomer, respectively. Sample and typical spectral conditions are given in the captions of Figures 1 and 2. For all tautomers except the aldehyde, each integrated intensity was taken as the product of the peak height and the line width of the best-fit Lorentzian curve obtained from a computer fit of the spectra processed with 0.5-Hz digital broadening (see Figure 1). For the aldehyde, the time-domain spectra were reprocessed with 10-Hz digital broadening (see Figure 2); the integrated intensities of the aldehyde, β-furanose, and β-pyranose resonances, together with the proportions of the latter two obtained from the spectra with 0.5-Hz digital broadening, yielded the proportion of aldehyde. Estimated precision, as a *percentage of the given value*, is ±2 for αP and βP, ±10 for αF and βF, and ±25 for CHO and $CH(OH)_2$. [b] pH 4.8. [c] Not detected. [d] pH 6.0.

Acknowledgment. This work was supported by the National Science Foundation (Grant PCM 83-04699) and the National Institutes of Health (Grant GM 22620). We thank Robert E. Addleman and Deon Osman for their help.

(19) Hayward, L. D.; Angyal, S. J. *Carbohydr. Res.* **1977**, *53*, 13-20.
(20) Angyal, S. J.; Pickles, V. A. *Aust. J. Chem.* **1972**, *25*, 1711-1718.
(21) Mazurek, M.; Perlin, A. S. *Can. J. Chem.* **1963**, *41*, 2403-2411.
(22) Cooper, J. W. *Comput. Chem.* **1976**, *1*, 55-60.
(23) Cooper, J. W. *J. Magn. Reson.* **1976**, *22*, 345-357.
(24) Cooper, J. W.; Mackay, I. S.; Pawle, G. B. *J. Magn. Reson.* **1977**, *28*, 405-415.
(25) Shaka, A. J.; Barker, P. B.; Bauer, C. J.; Freeman, R. *J. Magn. Reson.* **1986**, *67*, 396-401.
(26) Shaka, A. J.; Keeler, J. *Progr. NMR Spectrosc.* **1987**, *19*, 47-129. See section on cyclic sidebands caused by WALTZ-16 proton decoupling.

Nitrogen-15-Labeled Oligodeoxynucleotides. Characterization by ^{15}N NMR of d[CGTACG] Containing $^{15}N^6$- or $^{15}N^1$-Labeled Deoxyadenosine†

X. Gao and R. A. Jones*

Department of Chemistry
Rutgers, The State University of New Jersey
Piscataway, New Jersey 08855
Received January 26, 1987

The use of nitrogen NMR to probe DNA structure has been limited by the quadrupolar nature of the most abundant isotope of nitrogen, ^{14}N, and by the insensitivity and low natural abundance (0.37%) of the spin-$^1/_2$ isotope, ^{15}N.[1] We recently developed a synthetic route for the transformation of deoxyadenosine into both the $^{15}N^6$ and $^{15}N^1$ derivatives.[2] We now report the first syntheses of ^{15}N-labeled oligonucleotides and the first examples of the use of ^{15}N NMR to monitor and to characterize an oligonucleotide helix-to-coil transition.

The syntheses of d[CGT($^{15}N^1$)ACG] and d[CGT($^{15}N^6$)ACG] were carried out by a large-scale phosphoramidite prodecure similar to that reported previously.[3] In the present work, however, the 2-cyanoethyl group was used as the phosphate triester protecting group,[4,5] and deoxyadenosine (^{15}N labeled) was N protected

† Preliminary accounts of this work were presented at the Fourth Conversation in Biomolecular Stereodynamics, Albany, NY, June 1985, and at the VIIth International Round Table on Nucleosides, Nucleotides, and Their Biological Applications, Konstanz, W. Germany, Oct. 1986.

(1) Kanamori, K.; Roberts, J. D. *Acc. Chem. Res.* **1983**, *16*, 35-41.
(2) Gao, X.; Jones, R. A. *J. Am. Chem. Soc.* **1987**, *109*, 1275-1278.
(3) Gaffney, B. L.; Marky, L. A.; Jones, R. A. *Biochemistry* **1984**, *23*, 5686-5691.
(4) McBride, L. J.; Caruthers, M. H. *Tetrahedron Lett.* **1983**, *24*, 245-248.

0002-7863/87/1509-3169$01.50/0

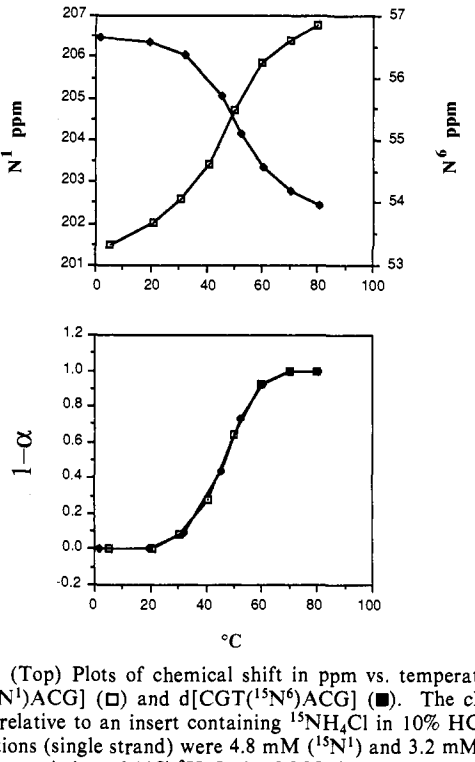

Figure 1. (Top) Plots of chemical shift in ppm vs. temperature for d[CGT(^{15}N^1)ACG] (□) and d[CGT(^{15}N^6)ACG] (■). The chemical shifts are relative to an insert containing $^{15}NH_4Cl$ in 10% HCl. The concentrations (single strand) were 4.8 mM (^{15}N^1) and 3.2 mM (^{15}N^6) in a buffer consisting of 20% ^2H_2O, 0.1 M NaCl, 10 mM NaH_2PO_4/$NaHPO_4$, 0.1 mM EDTA, pH 6.5. Spectra were obtained on a Varian XL-400 spectrometer in this department. (Bottom) Plots of $1 - \alpha$ vs. temperature for d[CGT(^{15}N^1)ACG] (□) and d[CGT(^{15}N^6)ACG] (■).

as the dibenzoyl derivative.[6,7] Purification by HPLC and base composition analysis by enzymatic degradation were carried out as reported previously.[3,8] A total of 13.2 μmol (760 OD_{260}) of the ^{15}N^1 hexamer and 8.7 μmol (500 OD_{260}) of the ^{15}N^6 hexamer were obtained. The molecule d[CGTACG] was chosen for this work because it already has been well characterized by a variety of experimental techniques including ^{1}H NMR.[8-11] In particular, d[CGTACG] has been shown to undergo a two-state melting transition.[11] Although these ^{15}N labels, by definition, are local structural monitors, in a molecule which has a two-state transition a local monitor can give results identical with those obtained by global techniques. Before using ^{15}N NMR to probe more complex structural changes, we wanted to see whether, using ^{15}N NMR, we could reproduce the known thermodynamic properties of a simple, two-state molecule.

The ^{15}N chemical shifts of both of the hexamers, of d(^{15}N^1)A and of d(^{15}N^6)A, were recorded over the temperature range of ~5 to 80 °C (Table I, supplemental material). In each case, only a single ^{15}N resonance was observed. When plotted as a function of temperature, the monomer chemical shifts show a linear temperature dependence (not shown), while the hexamers display the sinusoidal curve typical of a helix-to-coil transition (Figure 1). Duplex formation is accompanied by an upfield shift of ~2.6 ppm for the N^1 resonance and a downfield shift of ~1.2 ppm for the N^6 resonance. These chemical shift changes were measured relative to base lines drawn by extrapolation of the two highest and two lowest temperature points. To a good approximation, these points are in the (presumably) linear regions above and below the melting transition (≥70 or ≤21 °C). The magnitude and the direction of these ^{15}N chemical shift changes are consistent with the results of previously reported monomer and polymer studies.[12-14]

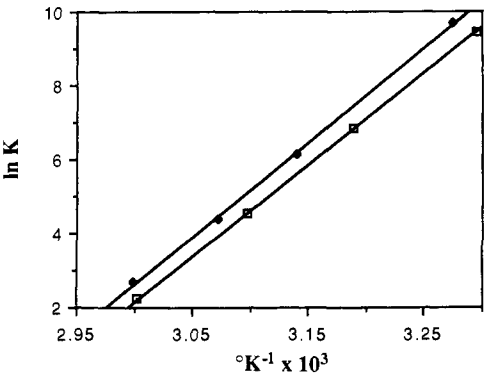

Figure 2. Plots of ln K vs. inverse temperature for d[CGT(^{15}N^1)ACG] (□) and d[CGT(^{15}N^6)ACG] (■), determined from[11] $K = \alpha/2(1 - \alpha)^2C_T$.

Table I

source	T_m (4 mM), °C	$\Delta H°$, kcal/mol	$\Delta S°$, kcal/deg mol
^{15}N^1	46	−49	−0.14
^{15}N^6	48	−51	−0.15
UV[8]	50	−46	−0.13
calmtrc[11]	51	−49	−0.15
pred[15]	40	−43	−0.13

A better comparison of the ability of these two ^{15}N resonances to monitor the helix-to-coil transition can be obtained by plotting $(1 - \alpha)$, where α is the fraction of single strands in the duplex state, vs. temperature, also shown in Figure 1. The quantity $1 - \alpha$ can be determined from the ratio of the change in chemical shift at a given temperature (relative to the low temperature base line) to the chemical shift difference between the duplex (low-temperature base line) and single strand (high-temperature base line) at that temperature, assuming that the percent change in chemical shift is proportional to the fraction of duplex present and that the transition is two-state. The equilibrium constant for duplex formation at a given temperature, once again assuming a two-state transition, may then be calculated.[11] Plots of ln K vs. T^{-1} (Figure 2) allow the melting temperature (T_m), $\Delta H°$, and $\Delta S°$ to be calculated (Table I).[11] Inspection of these thermodynamic data indicates that the values determined in this way by ^{15}N NMR are in excellent agreement with those derived from optical melting studies[8] or measured directly by calorimetric techniques[11] and with those predicted from the sum of nearest-neighbor interactions.[15] It should be noted that the optical and calorimetric work was done in 1 M NaCl, while the ^{15}N NMR was done in 0.1 M NaCl. This difference in salt concentration should not significantly affect the $\Delta H°$, and the small change in $\Delta S°$ would not be detectable at this level of accuracy. The T_m, however, should be a few degrees lower in the lower salt, as was observed. Thus ^{15}N NMR of an ^{15}N-labeled oligonucleotide is able to characterize accurately a two-state helix-to-coil transition. Of course, more examples will be necessary to establish the generality of this observation. Moreover, it should be emphasized that the most valuable applications of this approach are likely to lie in the study of structural changes occurring in large, non-two-state molecules or other more complex interactions, where the ^{15}N can function as a unique, local probe.

The spin–lattice relaxation times were determined by the inversion recovery method (Table II, supplementary material). At any given temperature a hexamer ^{15}N resonance relaxes faster

(5) Sinha, N. D.; Biernat, J.; Köster, H. *Tetrahedron Lett.* **1983**, *24*, 5843–5846.
(6) Takaku, H.; Morita, K.; Sumiuchi, T. *Chem. Lett.* **1983**, 1661–1664.
(7) Jones, R. A. In *Oligonucleotide Synthesis*; Gait, M. J., Ed.; IRL Press: Washington, DC, 1984.
(8) Kuzmich, S.; Marky, L. A.; Jones, R. A. *Nucleic Acids Res.* **1982**, *10*, 6265–6271.
(9) Clore, G. M.; Gronenborn, A. M. *EMBO J.* **1983**, *2*, 2109–2115.
(10) Clore G. M.; Gronenborn, A. M. *FEBS Lett.* **1984**, *172*, 219–225.
(11) Breslauer, K. J. In *Thermodynamic Data for Biochemistry and Biotechnology*; Springer-Verlag: W. Germany, 1986; pp 402–427.
(12) Poulter, C. D.; Livingston, C. L. *Tetrahedron Lett.* **1979**, 755–758.
(13) Dyllick-Brenzinger, C.; Sullivan, G. R.; Lang, P. P.; Roberts, J. D. *Proc. Natl. Acad. Sci. U.S.A.* **1980**, *77*, 5580–5582.
(14) James, T. L.; James, J. L.; Lapidot, A. *J. Am. Chem. Soc.* **1981**, *103*, 6748–6750.
(15) Breslauer, K. J.; Frank, R.; Blocker, H.; Marky, L. A. *Proc. Natl. Acad. Sci. U.S.A.* **1986**, *83*, 3746–3750.

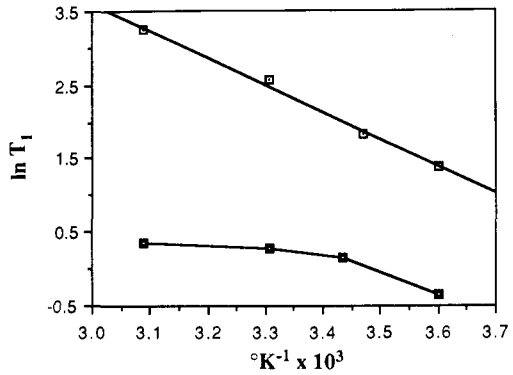

Figure 3. Plots of ln T_1 vs. inverse temperature for d[CGT(^{15}N^1)ACG] (■) and d(^{15}N^1)A (□).

than the corresponding monomer ^{15}N resonance, and the N^6 relaxes faster than the N^1 for both the hexamer and the monomer. The N^6, with two directly bonded protons, undergoes efficient ^{15}N–^{1}H dipolar relaxation. For example, a greater than 4-fold increase in the d(^{15}N^6)A T_1 was observed on changing the solvent to 100% D_2O. The N^1, which lacks a directly bonded proton, may have a more complicated relaxation mechanism. Pyridine ^{15}N relaxation occurs by a combination of dipolar, chemical shift anisotropic, and spin–rotation interactions,[16] each of which, by analogy, could be significant for the deoxyadenosine N^1. However, the contribution of spin–rotation relaxation in this case was shown to be negligible by the linear relationship between ln T_1 and T^{-1} for d(^{15}N^1)A, shown in Figure 3. The spin–rotation relaxation rate, unlike both the dipolar and chemical shift anisotropic relaxation rates, *increases* with temperature. The result for pyridine is that plots of ln T_1 vs. T^{-1} are nonlinear.[16] In an extreme case such as *n*-butyl nitrite, where spin–rotation relaxation predominates over the entire temperature range observed, such a plot is once again linear but has an opposite (positive) slope. Spin–rotation relaxation is most important for small molecules at high temperature,[16-19] and it therefore may not be surprising that it does not contribute to relaxation of the deoxyadenosine N^1.

Figure 3 also shows a plot of ln T_1 vs. T^{-1} for the ^{15}N^1 hexamer relaxation times. In this case the nonlinearity displayed is most likely a result of the changes in size and shape of the molecule which accompany the helix-to-coil transition. The rotational correlation time, τ_r, and hence the relaxation rate, are directly related to both size and shape.[10,18,19] In the duplex state the hexamer has approximate dimensions of 24 × 24 × 20.4 Å and can be treated as a sphere.[10] The single strand is not necessarily well described by a sphere at all and certainly not by a sphere of the same radius as the duplex. Thus, from these limited data, it appears that the ^{15}N T^1 also may be used to follow oligonucleotide structural changes.

We have shown for the first time that ^{15}N NMR of an oligonucleotide specifically ^{15}N labeled at either an H-bond acceptor nitrogen (N^1) or an H-bond donor nitrogen (N^6) is a sensitive structural monitor. Moreover, the T_m and thermodynamic data obtained for the helix-to-coil transition from the ^{15}N NMR agree well with those obtained by other methods. Unlike most other methods, however, ^{15}N NMR of specifically labeled molecules has the potential to probe otherwise inaccessible local structural phenomena in large molecules. These could range from thermally induced local melting, and the behavior of mismatched base pairs, to the structural changes that accompany enzyme recognition or drug binding.

Acknowledgment. Support of this work by grants from the National Institutes of Health (GM31483), the American Cancer Society (CH248B), and a Faculty Research Award to R.A.J. from the American Cancer Society is gratefully acknowledged. The XL-400 NMR was purchased in part with a grant from the National Science Foundation (CHEM-8300444). We are further indebted to Professors Arthur Pardi and Kenneth Breslauer of this department for many helpful discussions and valuable suggestions.

Supplementary Material Available: Tables of ^{15}N^1 chemical shifts, ^{15}N^6 chemical shifts, and ^{15}N relaxation times (2 pages). Ordering information is given on any current masthead page.

(16) Schweitzer, D.; Speiss, H. W. *J. Magn. Reson.* **1974**, *15*, 529–539.
(17) Lambert, J. B.; Netzel, D. A. *J. Magn. Reson.* **1977**, *25*, 531–538.
(18) Farrar, T. C.; Becker, E. D. In *Pulse and Fourier Transform NMR*; Academic: New York, 1971; pp 46–65.
(19) Levy, G. C.; Lichter, R. L. In *Nitrogen-15 Nuclear Magnetic Resonance Spectroscopy*; Wiley: New York, 1979.

Nickel-Containing CO Dehydrogenase Catalyzes Reversible Decarbonylation of Acetyl CoA with Retention of Stereochemistry at the Methyl Group

Scott A. Raybuck,† Neil R. Bastian,† Lynne D. Zydowsky,‡ Koji Kobayashi,‡ Heinz G. Floss,‡ William H. Orme-Johnson,† and Christopher T. Walsh*†

Department of Chemistry, MIT Cambridge, Massachusetts 02139
Department of Chemistry, The Ohio State University Columbus, Ohio 43210

Received January 20, 1987

Acetogenic and methanogenic bacteria can grow chemolithoautotrophically on CO_2 and H_2.[1] They do not have a number of the common carboxylases and thus make acetate by a distinctive route from two one-carbon fragments. A large body of incisive experimental work[2-6] has demonstrated that the methyl group of acetate in acetogens derives from N_5-methyltetrahydrofolate and that the carboxyl group of acetate derives from carbon monoxide, generated from CO_2 at the active site of the enzyme CO dehydrogenase. This enzyme appears to be the catalyst for C–C bond formation.

CO dehydrogenase has been best characterized from the acetogenic *Clostridium thermoaceticum*[7-9] where it is an $\alpha_3\beta_3$ structure containing zinc, iron–sulfur clusters, and tightly bound nickel ions. The nickel site of this metalloenzyme is incompletely characterized but will bind CO as detected by ^{13}CO hyperfine broadening of the ^{61}Ni EPR signal,[10] and the nickel site may be part of a mixed iron–nickel cluster.[11] This air-sensitive enzyme is routinely assayed anaerobically by CO dehydrogenation to CO_2 with passage of electrons to the artificial electron acceptor methylviologen, but it also catalyzes two mechanistically diagnostic isotope exchange reactions: (a) a *CoA ⇌ acetyl-*CoA exchange, suggesting a reversibly formed acetyl enzyme and (b) an exchange of *CO ⇌ *acetyl-CoA (carbonyl group).[12] The latter led Wood and colleagues[9] to propose an additional cleavage between the acetyl C_2–C_1 bond, producing a species with CH_3, CO, and SCoA

†MIT.
‡The Ohio State University.

(1) For a review, see: Wood, H. G.; Ragsdale, S. W.; Pezacka, E. *Biochem. Int.* **1986**, *12*, 421.
(2) Drake, H. L.; Hu, S.-I.; Wood, H. G. *J. Biol. Chem.* **1981**, *256*, 11137.
(3) Diekert, G. B.; Thauer, R. K. *J. Bacteriol.* **1978**, *136*, 597.
(4) Hu, S.-I.; Drake, H. L.; Wood, H. G. *J. Bacteriol.* **1982**, *149*, 440.
(5) Ljungdahl, L. G.; Wood, H. G. In *Vitamin B12*; Dolphin, D., Ed.; Wiley: New York, 1982; Vol. 2; pp 165–202.
(6) Hu, S.-I.; Pezacka, E.; Wood, H. G. *J. Biol. Chem.* **1984**, *259*, 8892.
(7) Drake, H. L.; Hu, S.-I.; Wood, H. G. *J. Biol. Chem.* **1980**, *255*, 7174.
(8) Ragsdale, S. W.; Clark, J. E.; Ljungdahl, L. G.; Lundie, L. L.; Drake, H. L. *J. Biol. Chem.* **1983**, *258*, 2364.
(9) Ragsdale, S. W.; Wood, H. G. *J. Biol. Chem.* **1985**, *260*, 3970.
(10) Ragsdale, S. W.; Ljungdahl, L. G.; DerVartanian, D. V. *Biochem. Biophys., Res. Commun.* **1983**, *115*, 658.
(11) Ragsdale, S. W.; Wood, H. G.; Antholine, W. E. *Proc. Natl. Acad. Sci. U.S.A.* **1985**, *82*, 6811.
(12) We have found, however, that the stabilities (with respect to oxygen and storage) of the two enzyme activities are *not* complementary and a positive CO ⇌ CO_2 assay by no means ensures the enzyme is capable of C–C bond formation and cleavage. Raybuck, S. A.; Bastian, N. R.; Orme-Johnson, W. H.; Walsh, C. T., manuscript in preparation.

0002-7863/87/1509-3171$01.50/0